

# Chebyshev Pseudospectral Solution of Second-Order Elliptic Equations with Finite Element Preconditioning

M. DEVILLE

*Unité de Mécanique Appliquée, Université Catholique de Louvain,  
B-1348 Louvain-la-Neuve, Belgium*

AND

E. MUND

*Service de Métrologie Nucléaire, Université Libre de Bruxelles,  
B-1050 Bruxelles, Belgium and  
Unité de Thermodynamique, Université Catholique de Louvain,  
B-1348 Louvain-la-Neuve, Belgium*

Received January 3, 1984; revised October 29, 1984

A new Chebyshev pseudospectral algorithm for second-order elliptic equations using finite element preconditioning is proposed and tested on various problems. Bilinear and biquadratic Lagrange elements are considered as well as bicubic Hermite elements. The numerical results show that bilinear elements produce spectral accuracy with the minimum computational work. *L*-shaped regions are treated by a subdomain approach. © 1985 Academic Press, Inc.

## 1. INTRODUCTION

This paper introduces a new type of preconditioning based on finite element algorithms in order to solve second-order elliptic partial differential equations by pseudospectral techniques.

It should be emphasized that the actual trends among numericists using spectral methods show a preference for pseudospectral approximations if Chebyshev solutions are sought. This is not very surprising as Chebyshev spectral methods (Galerkin or Tau techniques) are restricted to operators with constant coefficients and simple geometries (see, e.g., Orszag [1]). The extension of these spectral techniques to nonconstant coefficients, operators, and/or complicated geometries related to engineering problems would require huge computational resources and would strain the best algorithms on the best computers available at the present time. Consequently, it seems better and less expensive to resort to preconditioning methods within the framework of pseudospectral approximation, where variable coefficients, nonlinearities, etc., are more easily handled.

A recent paper by Haldenwang and co-authors [2] compares the Chebyshev

solution of Helmholtz equations by direct spectral solvers and iterative pseudospectral algorithms, based on finite difference preconditioning. This last technique to be very efficient requires excellent fast Poisson solvers using, for example, FFTs, cyclic reduction, multigrid procedures, etc. As finite element methods for elliptic equations are well developed and well designed, we propose as a natural extension of earlier work the use of finite elements as preconditioners of pseudospectral algorithms. By this coupling, we hope to accumulate the advantages of both techniques: variable coefficients in the differential operator and geometrical ease for the FE solver on one hand and accuracy for the spectral representation on the other hand.

Section 2 exposes the basic numerical method for self-adjoint second-order elliptic boundary value problems. Section 3 presents numerical results obtained for various problems on square and  $L$ -shaped regions. In the latter case, a subdomain technique is used for the spectral approximation. It is shown that Lagrangian bilinear elements provide a preconditioning technique which can compete with previous proposed algorithms [2, 3]. Spectral accuracy is obtained through a finite number of iterations and because of the very sparse structure of the matrix system resulting from the use of bilinear elements, this kind of preconditioning proves to be less expensive than pseudospectral solutions based on higher degree finite elements.

Direct solvers as in [2] lead to spectral accuracy with less computational effort for the same test problems. However the pseudospectral technique with finite element preconditioning forms a valuable tool of general capability which calls for further development to be able to tackle complex and nonlinear problems such as those encountered in fluid dynamics.

## 2. BASIC ALGORITHM

This section is devoted to the description of the general formalism. The basic idea rests upon an iterative process where at each step a problem of finite element type is solved with a right-hand side given by a residue evaluated through a Chebyshev pseudospectral calculation. The whole procedure may be viewed alternatively as a pseudospectral calculation with finite element preconditioning or as a series of finite element calculations with efficient pseudospectral corrective feedback. The expected accuracy depends essentially on the smoothness properties of the solution as well as on its spectral representation, i.e., on the cut-off value of the approximate expansion. A close relationship exists between this numerical procedure and the concept of iterated defect correction (IDeC) analyzed by Stetter (cf. [4]). This link will be investigated elsewhere.

For the sake of clarity we consider a 2-dimensional second-order differential equation with mixed homogeneous boundary conditions:

$$Lu(x, y) \equiv -\bar{\nabla}(p(x, y) \bar{\nabla}u(x, y)) + q(x, y) u(x, y) = f(x, y) \quad \forall x, y \in \Omega, \quad (1a)$$

$$a(x, y) \left( p \frac{\partial u}{\partial n} \right) + b(x, y) u = 0 \quad \forall x, y \in \Gamma. \quad (1b)$$

The domain  $\Omega$  is simply connected and bounded in the  $xy$  plane; its boundary  $\Gamma$  is piecewise smooth. The  $\bar{\nabla}$  symbol stands for the usual nabla operator whereas  $\partial/\partial n$  represents a normal derivative at each point of  $\Gamma$ , except possibly on a set of zero measure. We assume moreover, the following conditions of uniform ellipticity to be satisfied [5]:

$$p(x, y) \geq \gamma > 0, \quad q(x, y) \geq 0 \quad \forall x, y \in \Omega, \quad (2a)$$

$$a(x, y) + b(x, y) > 0 \quad \forall x, y \in \Gamma, \quad (2b)$$

ensuring problem (1) to be mathematically well-posed. Physically, the coefficients  $p(x, y)$  and  $q(x, y)$  represent a diffusion coefficient and an absorption term. In many practical situations these functions have piecewise analytic properties; throughout the sequel we shall assume however that  $p(x, y)$  and  $q(x, y)$  are continuously differentiable over  $\Omega$ .

With properties (2), a unique solution to problem (1) is known to exist among the set of functions having generalized derivatives of first-order square integrable over  $\Omega$ . Functions satisfying this property belong to the Sobolev space  $H^1(\Omega)$ . We introduce a scalar product  $(u, v)$  over elements of  $H^1(\Omega)$ :

$$(u, v) = \int_{\Omega} d\bar{r} u \cdot v. \quad (3)$$

Closely associated to Eqs. (1) is the scalar product  $B(u, v)$  induced by the energy norm

$$B(u, v) = \int_{\Omega} d\bar{r} (p \bar{\nabla} u \cdot \bar{\nabla} v + q uv) + \int_{\Gamma_e} d\bar{r}_s \cdot \frac{b}{a} uv, \quad \forall u, v \in H^1(\Omega), \quad (4)$$

where  $\Gamma_e$  is that part of the boundary where  $a(x, y) \neq 0$ . In its weak form, problem (1) may be reformulated in the following terms: find among  $H_0^1(\Omega) \subset H^1(\Omega)$ , the set of elements of the Sobolev space which satisfy the essential boundary conditions, the unique element  $u(x, y)$  such that

$$I(u) = \min_{v \in H_0^1(\Omega)} (B(v, v) - 2(f, v)). \quad (5)$$

For a second-order problem, the essential boundary conditions are only those which apply to the value of the function.

In the finite element approach of problem 1, one introduces a triangular or rectangular partition of  $\Omega$ ,  $\Omega_h$ , where  $h$  characterizes the "size" of the elements. A finite dimensional subspace of  $H_0^1(\Omega)$ ,  $S^N$ , is constructed with piecewise functions, usually polynomials of degree  $k$  and the variational formulation (5) is restricted to  $S^N$ , i.e., an element  $u_N \in S^N$  is sought such that

$$I(u^N) = \min_{v \in S^N} (B(v, v) - 2(f, v)). \quad (6)$$

Condition (6) leads to an  $N \times N$  algebraic system of equations which is symmetric, positive definite, and, because of the local character of the basis, banded:

$$L_{ap} \bar{u}_N = \bar{f}_N, \quad (7)$$

where  $L_{ap}$  is the stiffness matrix and  $\bar{u}_N$  denotes the vector of unknowns. Usual practice consists in solving Eq. (7) directly by performing first Cholesky factorization of the global stiffness matrix, followed by a double sweep on triangular systems. Finite element algorithms are extremely flexible with regard to the geometry of the problem. They are able to cope with complicated domains, the partitioning being most of the time made automatically by the computer code. Their accuracy depends essentially on the degree of the polynomial basis and on the nature of the problem. Classically one may show that for nonsingular problems—i.e., problems with smooth boundaries and interfaces—use of complete piecewise polynomials of degree  $(k - 1)$  on elements of size  $h$  yields an accuracy,

$$\|u - u_N\|_{0,\Omega} \leq ch^k |u|_{k,\Omega}, \quad (8)$$

for functions having  $k$ th order derivatives in the mean square sense. In inequality (8),  $c$  is a generic constant;  $\|u - u_N\|_{m,\Omega}$  and  $|u|_{m,\Omega}$  denote respectively the Sobolev norm and the seminorm of order  $m$  ([6]),

$$\|\phi\|_{m,\Omega}^2 = \sum_{|\alpha| \leq m} \int_{\Omega} d\bar{r} (D^{\alpha} \phi)^2, \quad (9a)$$

$$|\phi|_{m,\Omega}^2 = \sum_{|\alpha| = m} \int_{\Omega} d\bar{r} (D^{\alpha} \phi)^2, \quad (9b)$$

with, for 2D problems,

$$D^{\alpha} = \frac{\partial^{|\alpha|}}{\partial x^{\alpha_1} \partial y^{\alpha_2}}, \quad \alpha = (\alpha_1, \alpha_2), \quad |\alpha| = \alpha_1 + \alpha_2. \quad (9c)$$

As is well known, the result (8) is optimal. For nonsmooth boundaries or interfaces, however, the possible presence of singular functions at the vertices can sharply reduce the convergence orders for polynomial elements with degrees higher than one (cf. [7, 8]).

From here we shall concentrate on rectangular partitions of domains with boundaries parallel to the axes but otherwise arbitrary, the simplest case being the square  $\Omega_I = [-1, +1] \times [-1, +1]$ . More complicated domains such as the  $L$ -shaped domain sketched on Fig. 1 will usually be divisible into a set of adjacent rectangular subdomains ( $\Omega = \bigcup_{j=1}^J \Omega_j$ ), each of which is easily mapped onto the square  $\Omega_I$ . We shall also restrict this study to boundary value problems with regular solutions. The more general case of singular solutions is out of scope and deserves further attention.

We now turn to the Chebyshev pseudospectral approach of Problem 1, on  $\Omega_I$ .

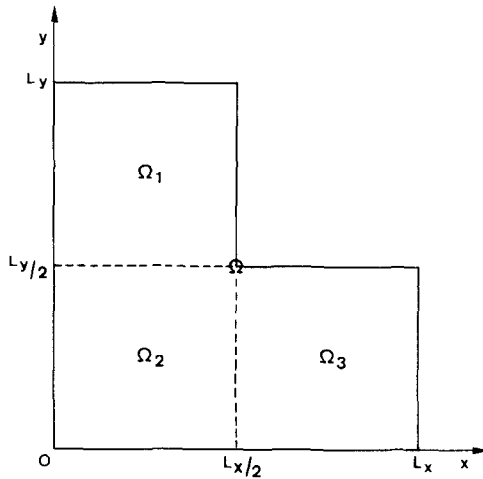


FIG. 1.  $L$ -shaped region divided in three subdomains  $\Omega_i$  ( $i = 1, 2, 3$ ).

This is an example of the weighted residual technique corresponding to orthogonal collocation within a set of global functions. Let  $\tilde{u}_N(x, y)$  and  $\tilde{f}_N(x, y)$  represent finite expansions in terms of Chebyshev polynomials of the solution and the righthand side of (Eq. 1a):

$$u(x, y) \sim \tilde{u}_N(x, y) = \sum_{i=0}^{N_x} \sum_{j=0}^{N_y} u_{ij} T_i(x) T_j(y) \quad (10a)$$

$$f(x, y) \sim \tilde{f}_N(x, y) = \sum_{i=0}^{N_x} \sum_{j=0}^{N_y} f_{ij} T_i(x) T_j(y) \quad (10b)$$

and

$$T_k(s) = \cos k\theta \quad (\cos \theta = s). \quad (10c)$$

The pseudospectral method applied on  $\Omega_i$  enforces the PDE to be satisfied at the internal nodes  $\{x_\alpha \otimes y_\beta; \alpha = 1, \dots, (N_x - 1); \beta = 1, \dots, (N_y - 1)\}$  of a Gauss-Chebyshev-Lobatto (GCL) quadrature rule. Accordingly the set of unknowns  $\{u_{ij}\}$  is determined such that

$$\iint_{\Omega_i} dx dy [L\tilde{u}_N - \tilde{f}_N] w_{\alpha\beta}(x, y) = 0 \quad \alpha = 1, \dots, (N_x - 1), \beta = 1, \dots, (N_y - 1), \quad (11a)$$

with

$$w_{\alpha\beta}(x, y) = \delta(x - x_\alpha) \delta(y - y_\beta) \quad (11b)$$

and

$$x_\alpha = \cos \frac{\alpha\pi}{N_x}, \quad y_\beta = \cos \frac{\beta\pi}{N_y}. \quad (11c)$$

The Chebyshev grid  $G_c$  is defined for  $0 \leq \alpha \leq N_x$  and  $0 \leq \beta \leq N_y$ . The coordinates (11c) of the 2D GCL quadrature rule correspond to the extrema of  $T_{N_x}(x) T_{N_y}(y)$ . The boundary conditions of problem 1 are taken into account by imposing their constraints into the physical space. Equations (11a) lead to an algebraic system in  $N = (N_x - 1)(N_y - 1)$  unknowns,

$$L_{\text{sp}} \hat{u}_N = \hat{f}_N, \quad (12)$$

where the vectors  $\hat{u}_N$  and  $\hat{f}_N$  contain the spectral coefficients  $\{u_{ij}\}$  and  $\{f_{ij}\}$  of (10).

The use of spectral and pseudospectral methods in computational fluid mechanics has been justified theoretically by many authors. An outline of basic convergence and stability results for time-dependent problems may be found in Gottlieb and Orszag [9]. The stability of the Fourier method for linear hyperbolic and parabolic PDEs with variable coefficients was studied by Kreiss and Oliger [10]. The essential result is that for problems with infinitely differentiable solutions, the approximation errors decay exponentially with  $N$ , the cut-off value of the expansion. More recently, Canuto and Quarteroni have analyzed the spectral and pseudospectral approximations of elliptic boundary value problems in a variational framework, typical of finite element theory (cf. [11, 12]). Briefly, they establish the convergence in weighted Sobolev norm for the Chebyshev pseudospectral approximation of a 1D diffusion–advection problem with variable coefficients and homogeneous Dirichlet boundary conditions, under fairly broad hypothesis: a Hölder continuity condition for the coefficients of the equation and a source term in a weighted Sobolev space  $H_\omega^\sigma$  ( $\sigma > \frac{1}{2}$ ). A similar result holds for the Neuman problem of the same equation with a diffusion coefficient identical to 1. The interested reader is referred to [12] for more details and in particular to Theorems 2.4 and 3.2 which are the main results. Similar properties for higher dimensional problems, although extremely plausible, are still an open question.

From a computational point of view the Chebyshev pseudospectral method is very attractive since it allows the use of FFT algorithms [13]. However, because of the global character of the expansions (10), the operator  $L_{\text{sp}}$  is a full  $N \times N$  matrix. The inversion of the algebraic system (12) may therefore be time-consuming. Additionally, the condition number  $\kappa(L_{\text{sp}})$  is  $O(N^4)$  and the system (12) is more and more ill-conditioned for increasing values of  $N$ . Both arguments led Orszag to propose the use of preconditioning techniques with sparse, easily invertible matrices such as those arising in finite difference calculations (cf. [1]).

Let  $Lu = f$  represent the basic boundary value problem (1) on the given domain  $\Omega$  and  $u^k$  an approximation of  $u$  at iteration  $k$  of an iterative process. Assuming the existence of the Fréchet derivatives of  $L$  we expand  $Lu$  into generalized Taylor

series in the neighborhood of  $u^k$  (cf. [14]). Truncating the series to first-order terms yields

$$Lu^k + \left. \frac{\partial L}{\partial u} \right|_{u^k} (u - u^k) \simeq Lu = f, \quad (13)$$

where  $\partial L/\partial u \triangleq L'$  is the Fréchet derivative of  $L$ . From (13), one obtains

$$L' \delta u^k = -R^k \quad (14a)$$

with

$$\delta u^k = u^{k+1} - u^k \quad (14b)$$

and

$$R^k = Lu^k - f. \quad (14c)$$

The residue of the basic equation at iteration  $k$ ,  $R^k$ , can be evaluated to a very high degree of accuracy (i.e., almost computer round-off) by use of Chebyshev series (10) in conjunction with fast inverse and direct Chebyshev transforms [13].

When  $L$  is a linear operator,  $L' = L$  and (14) becomes

$$L \delta u^k = -R^k. \quad (15)$$

Introducing  $L_{ap}$ , numerical approximation of  $L$ —namely the finite element matrix generated by condition (6)—into the left-hand side of Eq. (15), together with (14b) gives

$$u^{k+1} = (I - L_{ap}^{-1} L) u^k + L_{ap}^{-1} f, \quad k = 0, 1, \dots \quad (16)$$

This is essentially equivalent to the preconditioning with  $L_{ap}$  of the algebraic system (12). From a well-known theorem on the convergence of iterative methods, the algorithm (16) converges iff  $\rho(I - L_{ap}^{-1} L) < 1$ , where  $\rho(A)$  denotes the spectral radius of the matrix  $A$  [15]. It is also of common practice to underrelax iterative methods in order to stabilize the process and achieve convergence. The expression (14b) is then replaced by

$$\alpha \delta u^k = u^{k+1} - u^k \quad (17)$$

which transforms the iterative process (16) into the Richardson scheme:

$$u^{k+1} = (I - \alpha L_{ap}^{-1} L) u^k + \alpha L_{ap}^{-1} f, \quad k = 0, 1, \dots \quad (18)$$

The relaxation parameter  $\alpha$  is chosen in order to minimize  $\rho(I - \alpha L_{ap}^{-1} L)$ . Assuming the eigenvalues of  $L_{ap}^{-1} L$  to be real, simple and located into the interval  $[m, M]$ , it is well known that a maximum rate of convergence is reached for  $\alpha_{opt} = 2/(m + M)$ .

The algorithm runs as follows. One starts by defining the finite element grid  $G_{FE}$  whose vertices include the collocation grid  $G_c$ :  $G_c \subseteq G_{FE}$ .

For a rectangular domain  $\Omega = [a, b] \times [c, d]$  and cut-off values  $N_x, N_y$ , the coordinates of the mesh points are given by (11c) with adequate scaling. More complicated domains such as the  $L$ -shaped domain of Fig. 1 are divided into rectangular subdomains each of which is covered with a Chebyshev grid (11c). Figure 2, for instance, displays the  $L$ -shaped domain divided into 3 regions with a grid corresponding in each subdomain to the Chebyshev polynomials  $T_8(x) T_8(y)$ . Globally, the whole set of points defines the finite element grid. The minimization of the variational functional (6) over  $S^N$  yields a first approximation, say  $u^0(x, y)$ , of the solution of problem (1).

Suppose that the iterative procedure is on its way and  $u^k(x, y)$  is known. The next step consists first in evaluating the residue (14c). This is performed, subdomain by subdomain, in three stages.

1. Using an inverse Chebyshev transform (DCT)<sup>-1</sup>, compute the coefficients  $u_{ij}^k$  of the Chebyshev expansion (10a) in the subdomain from its subset of nodal values  $\{u^k(x_\alpha, y_\beta)\}$  at the local Chebyshev grid (11c).
2. Evaluate the residue in Chebyshev space. For example, if  $L$  is the Laplacian operator, this stage evaluates as

$$R_{ij}^k = \frac{1}{c_i} \sum_{\substack{n=i+2 \\ n+\text{even}}}^{N_x} n(n^2 - i^2) u_{nj}^k + \frac{1}{c_j} \sum_{\substack{m=j+2 \\ m+\text{even}}}^{N_y} m(m^2 - j^2) u_{im}^k - f_{ij}$$

$$0 \leq i \leq N_x, \quad 0 \leq j \leq N_y, \quad (19)$$

with

$$c_0 = 2, \quad c_i = 1 \quad \forall i > 0.$$

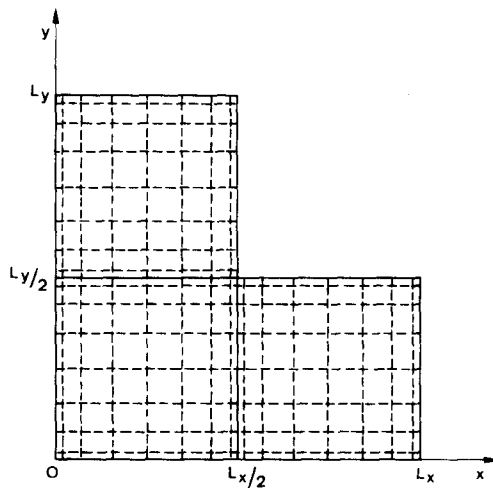


FIG. 2. Chebyshev collocation grids for the  $L$ -shaped region. In each subdomain,  $N_x = N_y = 8$ .



The residue evaluation might also be performed in physical space. However, this would imply a matrix multiplication (which can be vectorized on a supercomputer) with an operation count greater than the one involved in the DCT.

3. Using a direct Chebyshev transform DCT or a Clenshaw recurrence, restore the residue of a subdomain in physical space, i.e., evaluate the subset of nodal values  $\{R^k(x_\alpha, y_\beta)\}$  from the Chebyshev coefficients  $R_j^k$  of the subdomain.

Once these three stages are accomplished for all subdomains  $\Omega_j$  of  $\Omega$ , the global residue  $R^k(x, y)$  is projected onto  $S^N$  and one solves Eq. (15). This gives a correction  $\delta u^k(x, y)$  to  $u^k(x, y)$ . Setting

$$u^{k+1}(x, y) = u^k(x, y) + \alpha \delta u^k(x, y), \quad (20)$$

the iteration counter is incremented by one and the whole procedure is repeated—starting from the evaluation of the residues—until convergence is reached, i.e., when the ratio of residues in two successive steps  $|R^{k+1}/R^k|$  is greater than  $\frac{1}{2}$ .

At convergence, a final call to  $(\text{DCT})^{-1}$ , subdomain by subdomain, yields the set of Chebyshev coefficients  $\{u_{ij}^{\text{conv}}\}$  which allows the evaluation of  $u(x, y)$  everywhere in  $\Omega$ , in terms of the expansion (10a).

A few remarks are in order. We emphasize that, in the process of computing  $u^{k+1}(x, y)$  from  $u^k(x, y)$ , the partition  $\Omega_n$  remains unchanged. This is quite characteristic of IDeC and in sharp contrast with extrapolation methods. In the combined pseudospectral/finite element process, advantage is taken from both discretization methods. The high accuracy comes essentially from the collocation method, i.e., the residue calculation (19) in spectral space, provided the cut-off  $N$  is sufficiently high. Passing over from physical to Chebyshev space and vice versa is easily performed by fast transforms. In the finite element part, Cholesky factorization is made only once in a preprocessing stage. Subsequent iterations need only a forward and backward sweep with a computation time proportional to  $NW$  where  $W$  is the matrix bandwidth. Further time reductions may be obtained by the use of static condensation for elements with internal nodes and by gaussian quadrature. Chebyshev expansions represent global approximations, whereas finite elements are essentially local. In the subdomain approach where the residues are evaluated subdomain by subdomain, the  $C^\circ(\Omega)$  matching at interfaces provided by the finite elements is not sufficient to allow for spectral accuracy. One has to ensure the continuity of first-order derivatives at subdomain interfaces. In order to achieve such a requirement, the residues at interfaces are evaluated through a weak formulation of Eq. (15) leading to the relationship [16],

$$R^k(\partial_i \Omega) \triangleq \left[ \frac{\partial u^k}{\partial n} \right] \cdot \frac{1}{2\varepsilon}, \quad (21)$$

where the square bracket notation indicates the jump of normal derivatives at interfaces  $\partial_i \Omega$  and  $\varepsilon$  a boundary layer width typically of the order of the distance between the interface and the first interior point.

A final point remains for discussion: how to select the relaxation factor  $\alpha$ ? It is easy to show that for bilinear finite elements the extreme eigenvalues of  $L_{\text{ap}}^{-1}L$  are close to  $m = 1$  and  $M = \pi^2/4$ . Indeed, consider the 1D problem

$$-u''(x) = f(x) \quad x \in [-1, +1], \quad u(-1) = u(1) = 0, \quad (22)$$

where  $u$  and  $f$  are approximated by linear elements on the Chebyshev collocation grid. Defining  $h_j = x_{j+1} - x_j$ , one can easily compute the coefficients of the resulting tridiagonal matrix. It is found that, for the  $u_j$  variable, they are

$$a_{j,j-1} = -\frac{2}{h_{j-1}(h_{j-1} + h_j)}, \quad a_{j,j} = \frac{2}{h_j h_{j-1}}, \quad a_{j,j+1} = -\frac{2}{h_j(h_j + h_{j+1})}. \quad (23)$$

These coefficients are exactly the same as those produced by a finite difference (FD) approximation by centered differences on the Chebyshev grid. The difference between the two numerical techniques (FD and FE) will concern only the computation of right-hand side of the algebraic system, where finite differences involve only  $f_j$ , while finite elements require the contribution of  $f_{j-1}$ ,  $f_j$ ,  $f_{j+1}$ . The analysis carried out in Appendix 2 of Haldenwang *et al.* [2] within the finite difference context can therefore be transposed to the 1D finite element preconditioning and one concludes that for large cut-offs,  $m = 1$  and  $M = \pi^2/4$ . The extension to 2D problems is only approximate since with bilinear elements, one node interacts with its eight neighbors instead of four with finite differences. However, the difference should not be very significant and one concludes that with Lagrangian bilinear finite elements, the spectrum of  $L_{\text{ap}}^{-1}L$  should be close to that obtained with finite differences. Accordingly, the optimal relaxation factor  $\alpha_{\text{opt}}$  should be approximately equal to 0.577. Instead of using  $\alpha_{\text{opt}}$  from the start, another strategy consists in setting the initial guess  $\alpha^{\circ} = 1$  and adjusting the value at each iteration according to

$$\alpha^{k+1} = \max \left( \alpha_{\text{opt}}, \frac{2}{M^k + 1} \right), \quad (24)$$

where  $M^k$  is evaluated by the assumption  $\|\delta u^k\|/\|\delta u^{k-1}\| = |1 - \alpha^k M^k|$ .

### 3. NUMERICAL RESULTS

In this section, numerical results will be presented for several problems on square and  $L$ -shaped regions. Whenever possible, they will be compared with those provided in [2] with direct spectral and FD-pseudospectral solvers. It should be pointed out that in all the computations with FE preconditioning, the  $\alpha$  value was set systematically equal to 1.

The first problem is a Poisson equation with Dirichlet boundary conditions on the unit square  $[0, 1] \times [0, 1]$ . The solution is  $u = \sin(\pi/2)x \cos 2\pi y$ . Using  $N_x = N_y = 16$ , the Chebyshev representation is sufficient to achieve machine

accuracy. Figure 3 displays the evolution of the maximum absolute value of the spectral residue over all Chebyshev coefficients with respect to the iteration counter. It can be seen that spectral accuracy is reached within a finite number of iterations, which is smaller for a higher degree of the finite element interpolation ( $L_1, L_2$ : Lagrangian bilinear and biquadratic approximations respectively;  $H_3$ : bicubic Hermite). The number of iterations is always less than 10. The bicubic Hermite element does not perform better than the quadratic Lagrangian element.

The second test solves a Poisson equation with Dirichlet conditions, the solution of which is  $u = \sin 4\pi x \sin 4\pi y$ . Figure 4 shows the behavior of  $\max_{n,m} |R_{n,m}^k|$  as a function of the iteration index for various situations. With Lagrangian bilinear elements on a  $17 \times 17$  Chebyshev grid, we do not observe the typical spectral rate of convergence and the accuracy very quickly reaches an asymptotic level. A similar behavior occurs for Lagrangian biquadratic elements on the same grid. This phenomenon is due to the cut-off value, which is too low to allow machine accuracy. However, if the cut-off is increased to 32, both bilinear and biquadratic elements provide spectral accuracy within a few iterations ( $\leq 10$ ). The same figure shows the behavior of the spectral residue when finite differences replace finite

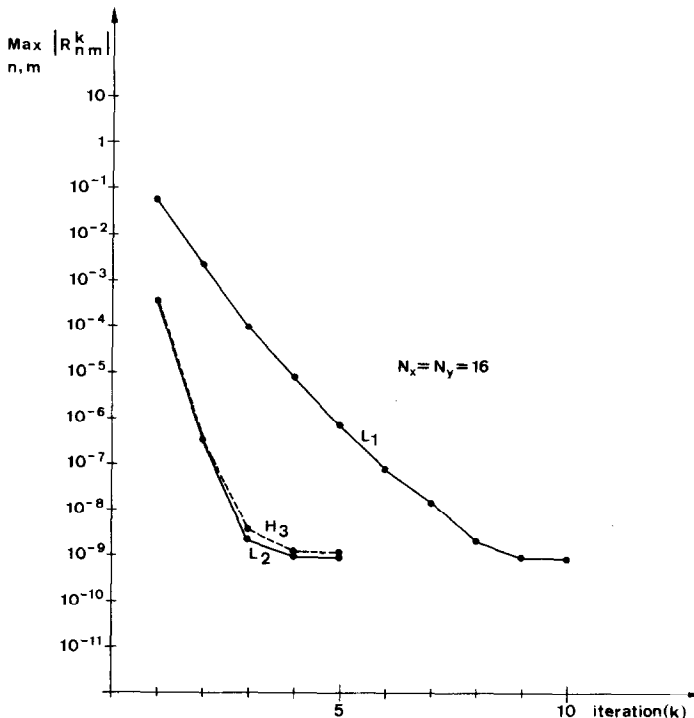


FIG. 3. Evolution of the maximum absolute value of the spectral residue with respect to the iteration index. The solution of the Poisson equation is  $u = \sin(\pi/2) x \cos 2\pi y$ .  $L_1, L_2$ , and  $H_3$  denote the use of Lagrangian bilinear, biquadratic, and bicubic Hermite elements in the preconditioning solver.

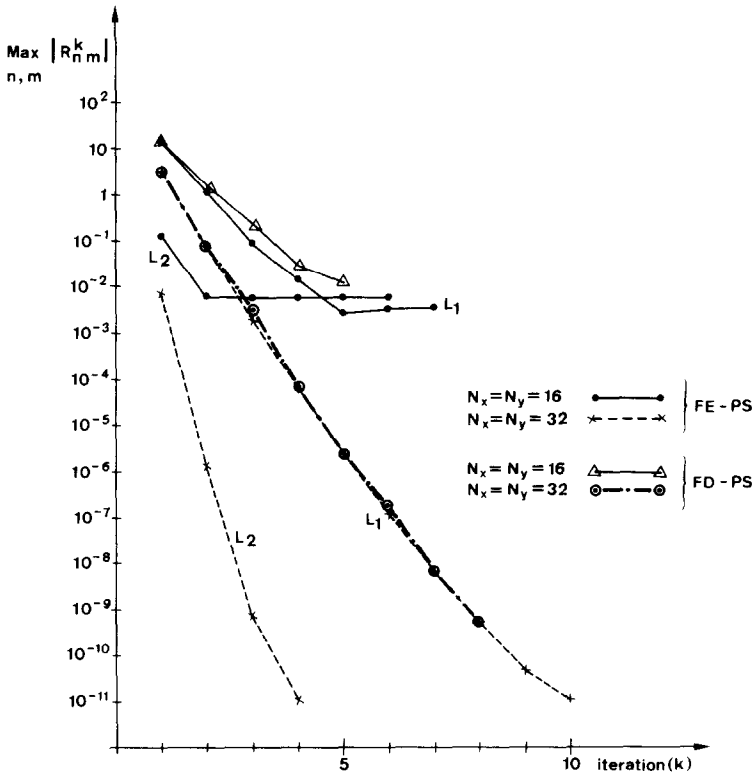


FIG. 4. See legend of Fig. 4. The solution of the Poisson equation is  $u = \sin 4\pi x \sin 4\pi y$ . FE-PS and FD-PS denote pseudospectral schemes with finite element and finite difference preconditioning, respectively.

elements in the preconditioning. Although the general trend is analogous, one can observe that the finite difference preconditioning is slightly less efficient as the stopping criterion is met earlier because the residue reduction is less impressive.

Figure 5 is related to problem (1) with  $p = 1 + 10x^2y^2$ ,  $q = 0$ . The solution is  $u = \sin \pi x \sin \pi y$ . The convergence achieved in 14 iterations is slowed down by the appearance of the nonconstant coefficients.

Finally, the fourth test was carried on the  $L$ -shaped region of Fig. 1, which is divided into three subdomains. Here, the solution  $u$  is  $\sin 2\pi x \sin 2\pi y$ . Figure 6 displays the evolution of  $\max_{n,m} |R_{n,m}|$  over all subdomains, in terms of the iteration parameter. With a  $16 \times 16$  Chebyshev expansion in each subdomain, the maximum residue decreases until  $10^{-10}$  where it reaches an asymptotic value. It can be seen that by (21) a patching of  $C^1$  continuity is achieved, providing the user with a solution of spectral accuracy.

Table I enlightens the comparison of the different preconditioners and several conclusions may be drawn.  $L_2$  and maximum norms are provided for the finite

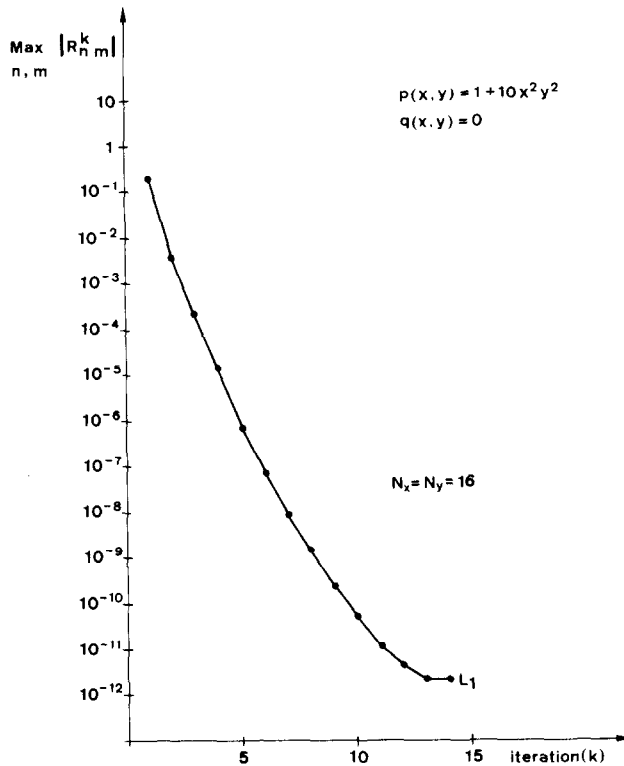


FIG. 5. Evolution of the maximum absolute value of the spectral residue with respect to the iteration index for a second-order elliptic equation with nonconstant coefficient.

element initial guess and the final pseudospectral solution. Table I also reports CPU times in seconds on an IBM 370/158 machine to compute the first finite element solution and the converged solution. In order to compare identical procedures, those CPU times were obtained using Clenshaw recurrence in the third stage of the residue evaluation, because for some types of elements,  $G_{FE}$  contains more points than  $G_c$ . The last column of Table I yields the CPU time of the direct solver [2], where the initial preprocessing of eigenvalues and eigenvector computation is included.

Despite the fact that the number of iterations is smaller for higher degree interpolants, the cost to attain machine precision with biquadratic or bicubic Hermite elements is greater than the cost needed by bilinear elements. This observation comes from the higher computational work involved in more accurate preconditioners. A further interesting conclusion is provided by the comparison of the pseudospectral  $16 \times 16$  solution with bilinear elements and the biquadratic finite element solution on a  $32 \times 32$  grid for the second problem. Both approximations attain the same level of accuracy in the maximum norm ( $\sim 10^{-6}$ ). However, the

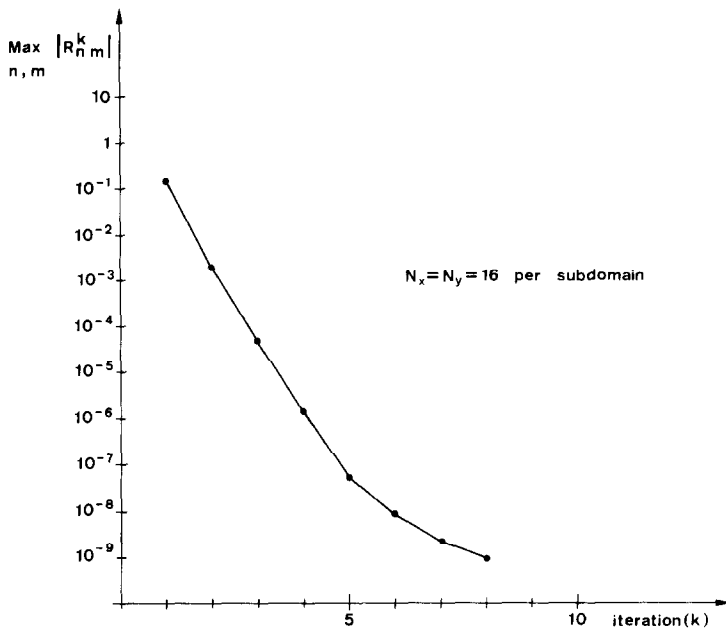


FIG. 6. Evolution of the maximum absolute value of the spectral residue with respect to the iteration index. The solution of the Poisson equation on the  $L$ -shaped domain of Fig. 1 is  $u = \sin 2\pi x \sin 2\pi y$ .

bilinear/pseudospectral solution costs five times less than the quadratic finite element solution. Consequently, *bilinear elements constitute the best preconditioning as they are able to reach spectral accuracy for the minimum cost.*

For the third test problem, the consumed CPU time is larger than for the first test case (constant coefficients) because the residue evaluation involves more back-and-forth transforms between real and Chebyshev spaces.

Another interesting comparison comes from Table II where the two preconditioners (FD and FE) are applied to the second test problem ( $u = \sin 4\pi x \sin 4\pi y$ ). Here, for the FD-pseudospectral (FDPS) scheme, the value of the parameter  $\alpha$  is computed through Eq. (24) and is always between 1 and 0.95.

Using bilinear finite elements, Clenshaw recurrence is replaced by direct Chebyshev transform DCT at stage 3 of the residue computation because in that case  $G_C \equiv G_{FE}$ .

For the  $17 \times 17$  case, both preconditioners offer the same accuracy at the same computing cost. For the  $33 \times 33$  discretization, the FE-pseudospectral scheme is approximately four times as expensive as the FDPS method. This difference is explained easily by the asymptotic operation counts which are  $N \log_2 N_y$  and  $NN_y$  for the FD and FE algebraic solvers, respectively. Note that the replacement of the Clenshaw algorithm by the Chebyshev transform leads to a reduction by a factor 6 of the computing time for the FE-pseudospectral computation. However, the good

TABLE I  
 Comparison of Different Types of Finite Element Preconditioning  
 with Respect to Accuracy and Computing times

	$\ u - u^{(0)}\ _2$	$\ u - u^{(\text{conv})}\ _2$	$\ u - u^{(0)}\ _\infty$	$\ u - u^{(\text{conv})}\ _\infty$	CPU $t$ , $u^{(0)}(s)$	CPU $t$ , $u^{(\text{conv})}(s)$	No. Iterations	CPU direct solver
$T_1^1(16, 16)$	2.27 (-3)	1.65 (-13)	8.21 (-3)	6.57 (-13)	4	91	10	
$T_2^1(16, 16)$	3.46 (-6)	2.54 (-14)	1.33 (-5)	7.76 (-14)	22	124	5	4.30
$T_3^1(16, 16)$	1.13 (-5)	8.07 (-14)	2.93 (-5)	2.35 (-13)	67	145	5	
$T_1^2(16, 16)$	3.07 (-2)	6.37 (-7)	9.88 (-2)	3.84 (-6)	4	54	6	4.30
$T_2^2(16, 16)$	4.40 (-4)	8.01 (-8)	1.71 (-3)	2.20 (-7)	22	75	3	4.30
$T_3^2(32, 32)$	8.29 (-3)	9.09 (-15)	2.82 (-2)	2.91 (-14)	38	554	11	23.4
$T_2^3(32, 32)$	2.30 (-5)	9.08 (-15)	8.25 (-5)	2.91 (-14)	261	1538	5	23.4
$T_1^3(16, 16)$	1.61 (-3)	3.78 (-15)	6.14 (-3)	6.95 (-15)	8	139	14	
$T_2^3(16, 16)$	1.99 (-3)	5.11 (-14)	7.06 (-3)	3.38 (-13)	2.4	288	8	

TABLE II  
 Comparison of Pseudospectral Schemes Using Finite Element and Finite Difference Preconditioning

Preconditioner	$\ \mu - \mu^{(0)}\ _2$	$\ \mu - \mu^{(\text{conv})}\ _2$	$\ \mu - \mu^{(0)}\ _\infty$	$\ \mu - \mu^{(\text{conv})}\ _\infty$	CPU $t$ $t^{(0)}$	CPU $t$ $t^{(\text{conv})}$	No. Iterations
FD (17 <sup>2</sup> )	3.60 (-2)	8.45 (-6)	1.10 (-1)	4.54 (-5)	1	10	5
FE (17 <sup>2</sup> )	3.07 (-2)	6.37 (-7)	9.88 (-2)	3.84 (-6)	4	9	6
FD (33 <sup>2</sup> )	8.35 (-3)	1.24 (-12)	2.59 (-2)	5.36 (-12)	3	23	8
FE (33 <sup>2</sup> )	8.29 (-3)	9.08 (-15)	2.82 (-2)	2.91 (-14)	37	93	11



performance of the cyclic-reduction solution is restricted to the treatment of separable elliptic equations while the finite element method has greater generality.

The numerical results obtained in this research show that with finite element preconditioning, one may reach spectral accuracy within a few iterations using a Chebyshev pseudospectral method, together with a discrete Chebyshev transform. It is shown that bilinear Lagrangian elements provide the required level of accuracy for the less expensive computing time. Further attention should be paid to the patching conditions at subdomain interfaces for more complicated geometries.

#### ACKNOWLEDGMENTS

We thank Dr. Y. Morchoisne from Department of Aerodynamics (ONERA-France) for valuable discussions and suggestions. E. M. acknowledges continuous financial support from the Fonds National de la Recherche Scientifique (FNRS).

#### REFERENCES

1. S. A. ORSZAG, *J. Comput. Phys.* **37** (1980), 70.
2. P. HALDENWANG, G. LABROSSE, S. ABBOUDI, AND M. DEVILLE, *J. Comput. Phys.* **55** (1984), 115.
3. TH. ZANG, Y. S. WONG, AND M. Y. HUSSAINI, "Spectral Multigrid methods for elliptic equations II," ICASE Report 172131, 1983, Hampton, Va.
4. H. J. STETTER, *Numer. Math.* **29** (1978), 425.
5. G. STRANG AND G. J. FIX, "An Analysis of the Finite Element Method," Series in Automatic Computation, Prentice-Hall, Englewood Cliffs, N.J., 1973.
6. P. G. CIARLET, "The Finite Element Method for Elliptic Problems," North-Holland, Amsterdam, 1979.
7. R. B. KELLOGG, in "Numerical Solution of Partial Differential Equations, II, Synspade, 1970" (B. Hubbard, Ed.), p. 351. Academic Press, New York, 1971.
8. J. P. HENNART AND E. H. MUND, *Nucl. Sci. Eng.* **62** (1977), 55.
9. D. GOTTLIEB AND S. A. ORSZAG, CBMS-NSF Regional Conference Series in Applied Mathematics Vol. 26, Soc. Indus. Appl. Math., Philadelphia, 1977.
10. H. O. KREISS AND J. OLIGER, *SIAM J. Numer. Anal.* **16** (1979), 421.
11. C. CANUTO AND A. QUARTERONI, *Math. Comput.* **38** (1982), 67.
12. C. CANUTO AND A. QUARTERONI, in "Proceedings of the Symposium on Spectral Methods for PDE" (R. G. Voigt, D. Gottlieb, and M. Y. Hussaini, Eds.), SIAM Monograph, Philadelphia, 1984.
13. M. DEVILLE AND G. LABROSSE, *J. Comput. Appl. Math.* **8** (1982), 293.
14. L. B. RALL, "Computational Solution of Nonlinear Operator Equations," Wiley, London, 1969.
15. L. A. HAGEMAN AND D. M. YOUNG, "Applied Iterative Analysis," Academic Press, London, 1981.
16. Y. MORCHOISNE, in "Proceedings of the Symposium on Spectral Methods for PDE" (R. G. Voigt, D. Gottlieb, and M. Y. Hussaini, Eds.), SIAM Monograph, Philadelphia, 1984.